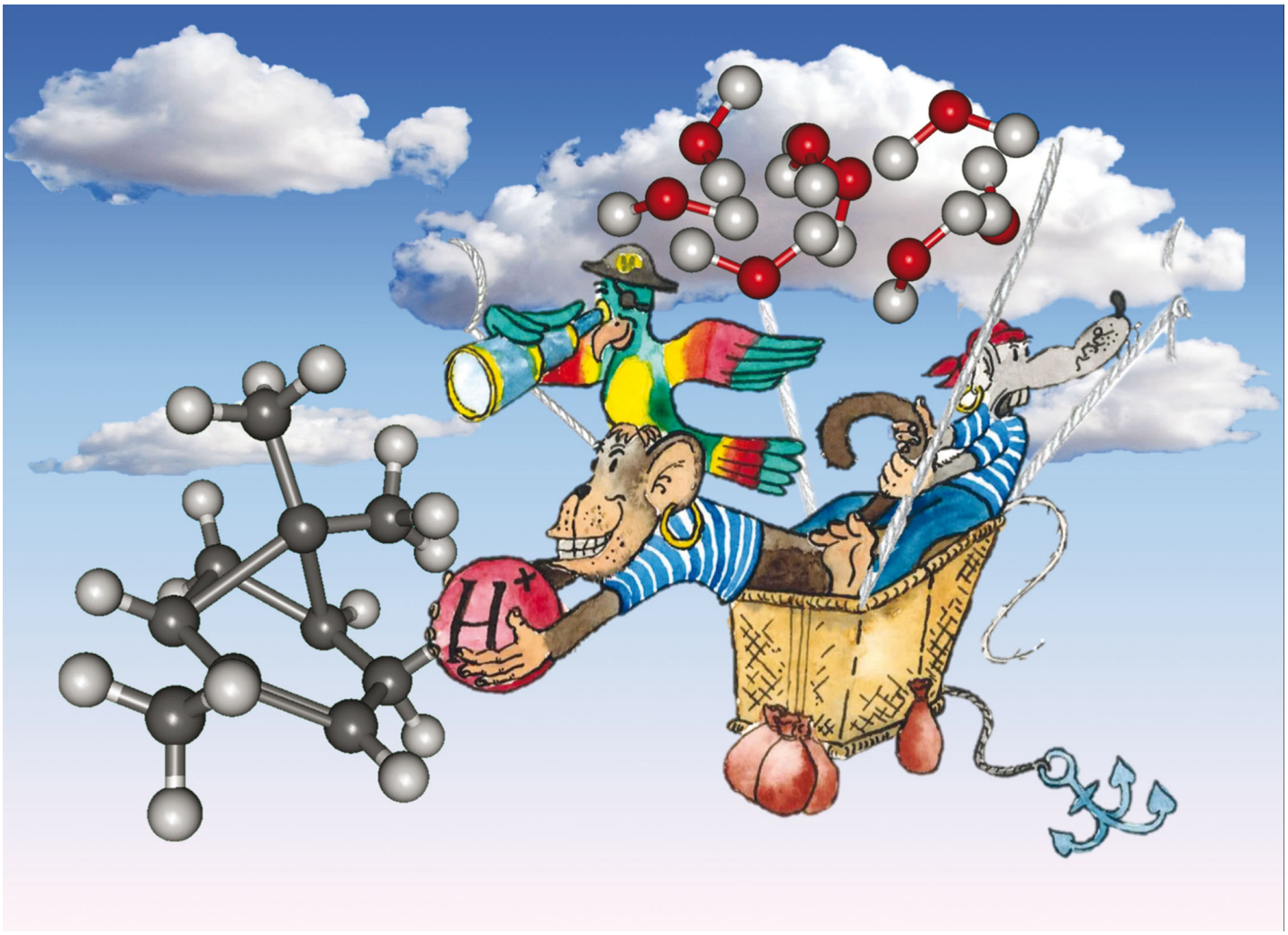

Showcasing research from the group of Molecular and Cluster Dynamics at J. Heyrovský Institute of Physical Chemistry at the Czech Academy of Sciences.

Proton transfer from pinene stabilizes water clusters

Direct ionization of water clusters is an exothermic process resulting in extensive water evaporation and formation of protonated water cluster cations. Here we show that the same cations may be formed by proton transfer from pinene. This process, however, depends on the solvation energy of the proton within the cluster. Only water clusters containing more than 7 water molecules are able to "steal" the proton from pinene as illustrated on the cover art. Such ionization is therefore gentle and results in thermodynamically stable water cluster cations. The studied mechanism may occur in the atmosphere.

As featured in:

See Petr Slavíček, Jaroslav Kočišek *et al.*, *Phys. Chem. Chem. Phys.*, 2019, **21**, 13925.

ROYAL SOCIETY OF CHEMISTRY | Celebrating IYPT 2019

rsc.li/pccp

Registered charity number: 207890

PCCP

PAPER

Cite this: *Phys. Chem. Chem. Phys.*, 2019, **21**, 13925

Proton transfer from pinene stabilizes water clusters†

Jan Poštulka,[a] Petr Slavíček, *[ab] Alicja Domaracka,[c] Andriy Pysanenko,[b] Michal Fárník [b] and Jaroslav Kočišek *[b]

Received 21st September 2018,
Accepted 19th November 2018

DOI: 10.1039/c8cp05959d

rsc.li/pccp

We ionize small mixed pinene–water clusters by electron impact or by using photons after sodium doping and analyze the products by mass spectrometry. Electron ionization results in the formation of pure pinene, mixed pinene–water and protonated water cluster cations. The "fragmentation free" photoionization after sodium doping results into the formation of only water–Na^+ clusters with a mean cluster size below that observed after electron ionization. We show that protonated water clusters are formed both directly and indirectly *via* pinene ionziation. The latter pathway is detailed by *ab intio* calculations, demonstrating the feasibility of proton transfer from pinene for larger water clusters. In small clusters, the proton transfer reaction is controlled by proton solvation energy and we can thus estimate its value for finite size clusters. The observed stabilization mechanism of water clusters may contribute to the formation of cloud condensation nuclei in the atmosphere.

1 Introduction

We explore the dynamics of pinene and mixed pinene–water clusters after ionization. Pinenes are primary constituents of pine resin. For the present study, we selected the more common of the naturally occurring pinenes – alpha pinene.[1] The pinene cluster dynamics after ionization is relevant for understanding the combustion chemistry of pinene, which has been proposed as a promising renewable fuel.[2] Ionic chemistry in mixed pinene–water clusters is then important for understanding the water addition effect on the plasma treatment of VOCs.[3] Pinene was used as a model compound to demonstrate so called "on-water" chemical reactions.[4] These reactions occur when water insoluble organics are placed on the surface of small water microdroplets. Heterogeneous neutral clusters prepared by adiabatic expansion into a vacuum in the present work provide an ideal substrate to study such weakly bound systems and explore the reactivity change within solvation.

Pinene is also an important biogenic emission in the atmosphere where it can form binary organic–water aerosols (*e.g.* ref. 5). The aerosol formation is usually explained through a neutral pathway, by degradation of volatile pinene to less volatile oxygenated molecules.[6,7] The nucleation rate in pinene rich atmospheres is however strongly dependent on the external ionization.[8] More recently, it has been shown that ionization is a necessary condition for the formation of critical condensation nuclei.[9] Nucleation also strongly correlates with humidity.[10,11] The question therefore arises if there can be also other ion based pathways of aerosol formation in pinene–water mixtures. We suggest that the stabilization of protonated water clusters by pinene, observed here, might provide an additional pathway to aerosol nucleation.

Our investigations show that water clusters are stabilized by proton transfer from ionized pinene. Proton transfer in heterogeneous water clusters has been extensively studied due to its importance in atmospheric chemistry (*e.g.* ref. 12 and 13) and biochemistry (*e.g.* ref. 14–16). Studied molecules often contain an oxygen atom as a competing hydrogen bond acceptor to that of water.[17,18] In such systems, similar to pure water clusters, proton transfer may be highly exothermic.[19,20] Particular focus was on the intra and intermolecular proton transfer mediated by water bridges,[21] even in systems containing only one water molecule.[22] Studies of proton transfer reaction in heterogeneous water clusters containing pure hydrocarbons were pioneered in the group of El Shall.[23] Proton trasfer to water in the ionic state was observed *e.g.* from an acetylene dimer.[24] However, we are not aware of any study of the ionization of mixed pinene–water clusters.

2 Methods

2.1 Experimental

The experimental part was conducted on the cluster beam (CLUB) setup.[20] The configuration of the molecular beam source was similar to that used in ref. 25. The pinene was

[a] *Department of Physical Chemistry, University of Chemistry and Technology, Technická 5, Prague 6, Czech Republic. E-mail: petr.slavicek@vscht.cz*
[b] *J. Heyrovský Institute of Physical Chemistry v.v.i., The Czech Academy of Sciences, Dolejškova 3, 18223 Prague, Czech Republic. E-mail: kocisek@jh-inst.cas.cz*
[c] *Normandie Univ., ENSICAEN, UNICAEN, CEA, CNRS, CIMAP, 14000 Caen, France*

† Electronic supplementary information (ESI) available: (1) High mass part of the mass spectra taken at conditions I and II; (2) calculated binding energies of pinene in mixed clusters; (3) binding energies from Fig. 2 calculated including dispersion correction; (4) Cartesian coordinates for structures in Fig. 2A and 5. Cartesian coordinates for structures in Fig. 2B. See DOI: 10.1039/c8cp05959d

Table 1 Expansion conditions used in the experiment. Expansion pressure P_e in Bar and temperatures in K of the pinene reservoir T_r, expansion nozzle T_n, water reservoir T_{wr}, sodium reservoir T_{NaR} and sodium pickup channel T_{NaC}. Alpha pinene was purchased from Sigma-Aldrich, with stated purity 98%

No.	I	II	III
Buffer	Ar	He	Ar
P_e	2	3	3.2
T_n	323	328	343
T_r	313	308	333
T_{wr}	—	303	303
T_{NaR}	—	—	457
T_{NaC}	—	—	463

evaporated in the oven and expanded into a vacuum through a 90 μm conical nozzle together with the buffer gas. To induce hydration, a water reservoir was added into the buffer gas line. The conditions used for preparation of different clusters are summarized in Table 1.

The molecular beam was probed ~1.5 m downstream from the nozzle. Two ionization approaches were used: (i) electron ionization (EI) and (ii) photoionization after sodium doping (NaPI).

For EI (i), we used the pulsed electron gun built into the TOF mass spectrometer. Control over the energy of electrons enables two types of measurements. Measurements of mass spectra at a single energy of electrons or 3D *m*/*z*-electron energy-intensity scans. In the 3D mode, we can extract the mass spectrum at defined energy or electron energy dependent ion yields. Details can be found in our previous publication.[26]

For NaPI (ii), clusters first pass through a sodium doping cell. Sodium atoms stick to the cluster. In water, a Na^+ and e^- ion pair is formed.[27–29] Ionization is then induced in the ionization region of the mass spectrometer by photo detachment of the solvated electron at 315 nm, below the ionization threshold of any of the cluster constituents. For some types of clusters, the technique was shown to be fragmentation free[27,30,31] and is also used to determine neutral cluster size distributions.[19,20] However, in mixed clusters and nanoparticles one has to be careful about the interaction with cluster constituents that can result in electron binding energy above the energy of the detection photon.[32–34] Details of the Na doping application on the CLUB setup can be found in ref. 35.

2.2 Simulations

We have investigated the stability of mixed clusters containing one pinene molecule and up to 8 molecules of water ($C_{10}H_{16}$-$(H_2O)_{n\leq 8}$). In the theoretical study, we have focused on the electron or proton transfer between pinene and water units. Therefore, we have included only a single pinene molecule in the simulations. First, we have mapped the relevant minima of the $C_{10}H_{16}(H_2O)_n$ and $C_{10}H_{16}(H_2O)_n^+$clusters, using the quenching approach. The molecular dynamics (MD) serves here as a tool for an efficient search for low-lying minima. We performed MD simulations of the respective clusters, using simulations with a constant temperature set to 500 K. The temperature was maintained with a Nosé–Hover thermostat. We have then minimized the structures from the MD simulations in regular intervals, performing 95 optimizations in total. For the minimum structures, we have calculated the binding energy for a water molecule in the cluster. This energy tells us how much energy is required to detach a water molecule from a water cluster connected with a pinene molecule. The binding energy was calculated as a difference between the energy of an optimized cluster of size n and a sum of the energy of the cluster of size $n-1$ and a water molecule. The MD simulations were run at the BLYP/6-31g* level with dispersion correction, and the cluster optimization was performed using the BMK functional[36] and 6-31++g** basis set. The BMK functional was used as a reliable and well tested functional with high fraction of exact exchange. In particular, we were afraid of artificial charge localization observed for molecular clusters, which is mitigated with the high fraction of exact exchange in the hybrid functionals.[37] The *ab initio* dynamics was run for 24 ps in each case (both for the neutral and ionized case). The length of the simulations is relatively limited, yet the high temperature allows for a reasonable sampling of the configuration space. We have opted for *ab initio* MD to avoid difficult parametrization for the two electronic states. The temperature used allowed for high flexibility of the system yet evaporation was still not observed within the relatively short duration of the simulation.

Next, we focused on the possible charge transfer processes following the pinene ionization. We considered two possible routes (i) electron transfer between pinene and a water cluster and (ii) proton transfer between the two units.

The energetics of the electron transfer mechanism was calculated with the use of the constrained density functional theory (CDFT).[38] This method allows for *ab initio* calculations with additional constraint on the charge distribution between different moieties. We can thus compare the energies of the clusters with charge localized on the pinene molecule $(C_{10}H_{16})^+(H_2O)_n$ or water cluster $C_{10}H_{16}(H_2O)_n^+$, using ground state density functional techniques. Here, we used the Hartree–Fock method and 6-31+g* basis set. After the proton transfer in the water unit took place, the resulting structures were then re-optimized without any constraint at the BMK/6-31++g** level.

Alternatively, we consider energetics for the proton transfer from the pinene cation into the water cluster. We first identified the C–H bond most susceptible to the deprotonation. This deprotonated pinene was then optimized with a protonated water cluster at the BMK/6-31++g** level. The energy necessary for the proton transfer process was evaluated as a difference between the energy of the deprotonated pinene – protonated water cluster system $C_{10}H_{15}(H_2O)_nH^+$ and the energy of the optimized structure of the pinene–water cluster $(C_{10}H_{16})^+(H_2O)_n$. All the *ab initio* calculations were performed in the Gaussian09 code[39] except for the auxiliary CDFT calculations and subsequent reoptimizations which were carried out in the Q-Chem 4.3 code.[40]

3 Results and discussion

The results are organized as follows. First we discuss the effect of the solvent water molecules on the molecular fragmentation.

Then we describe the pinene–water reactivity in the ionic state and finally we discuss the mechanism of the observed charge transfer.

3.1 Molecular fragmentation

Fig. 1 compares pinene cluster mass spectra after EI at two different expansion conditions I and II to the reference mass spectrum of the molecular pinene from the NIST database.[41] The mass spectrum of molecular (monomer) pinene is dominated by fragment $m/z = 93$ that was previously assigned to the protonated toluene formed by the loss of the central part of the molecule.[42] As expected, the fragmentation is suppressed in the clusters.[43–45] The inhibition of fragmentation is expressed especially by the pronounced parent ion peak at $m/z = 136$ in both spectra, which is almost missing in the molecular spectrum.[41] The two conditions I and II represent expansions where the primary neutral precursors are pinene clusters $(C_{10}H_{16})_k$ or mixed pinene–water clusters $(C_{10}H_{16})_m(H_2O)_n$, respectively. Even though the average number of pinene molecules within the pure clusters I is lower than the number of water molecules in the mixed clusters II ($k < n$), the protective effect is more pronounced in the pure clusters. We tentatively attribute this to the better energy transfer between the molecules of the same type, which enables energy redistribution prior to the fragmentation.

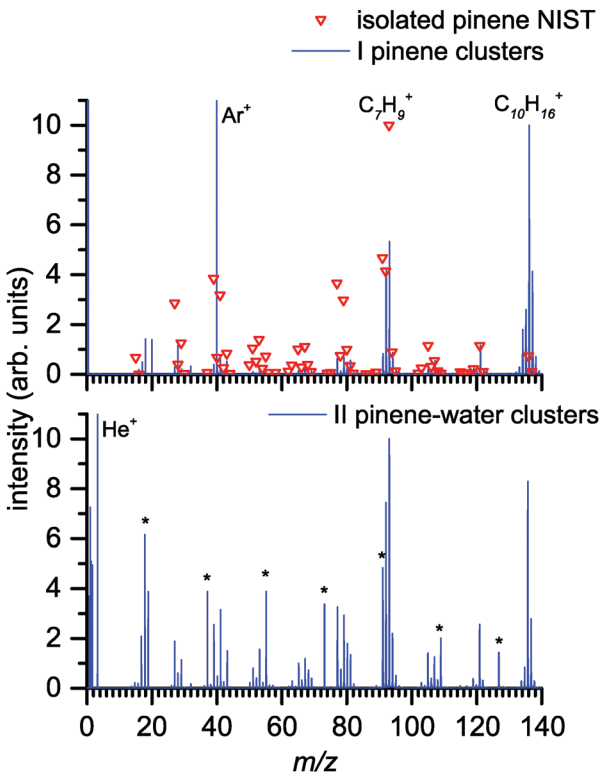

Fig. 1 Mass spectrum of pinene after EI taken from the NIST database[41] compared to the mass spectrum of pinene clusters I (top) and mass spectrum of mixed pinene–water clusters II (bottom) taken at the energy of electrons 70 eV. Ar and He were used as a buffer gas, respectively. Water cluster peaks are marked by asterisks. The presented low mass part of the spectra demonstrates the effect of the environment on the pinene fragmentation after EI. The high mass part is in the ESI.†

The lower protective effect of water in comparison to pinene molecules in the clusters may be also explained by weak interaction of pinene with water. Fig. 2 shows the optimized structures of the neutral pinene–water $C_{10}H_{16}(H_2O)_n$ clusters (A) and ionized $(C_{10}H_{16})^+(H_2O)_n$ clusters (B). Pinene is a non-polar, hydrophobic molecule[46] and this can be already demonstrated on the microscopic level. Water molecules tend to form aggregates among themselves, utilizing the potential of the strong hydrogen bonds. In fact, the water clusters are structurally not too different from isolated water clusters.[47] Therefore, the pinene–water clusters can be best described as a pinene molecule weakly interacting with water clusters.

Finally, the lower protective effect of water can be based on the reactivity of the studied species in the ionic state. An important stabilization mechanism in hydrocarbon clusters is

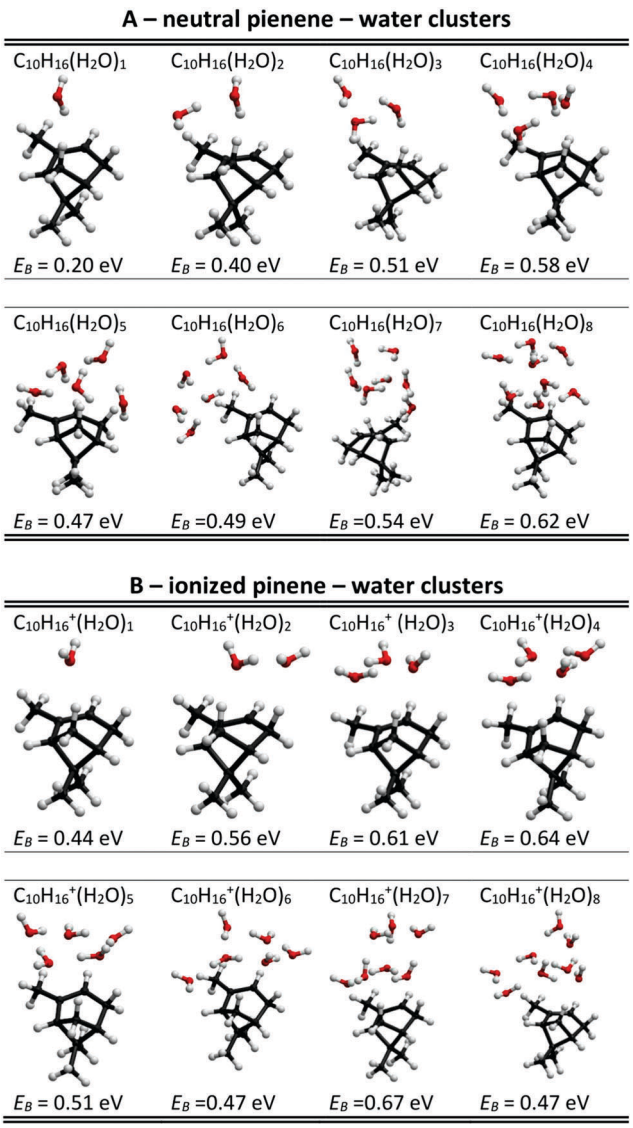

Fig. 2 Calculated structures of the (A) neutral and (B) ionized pinene–water clusters, optimized at the BMK/6-31++g** level. E_B are water binding energies for the nth water in the (A) $C_{10}H_{16}(H_2O)_n$ or (B) $C_{10}H_{16}^+(H_2O)_n$ clusters calculated at the same level of theory.

proton transfer. It appears from the present experiment that the relative abundance of the protonated pinene monomer is higher in the case of pure clusters (conditions I) than in the case of mixed clusters (conditions II). The corresponding ratios of the integrated ion yields at the mass of pinene (m/z = 136) to that of protonated pinene (m/z = 137) are $Y_{136/137}$ = 1.8 in the case of pure clusters and $Y_{136/137}$ = 2.8 in the case of mixed clusters. We show below that the observed decrease of protonated pinene abundance is caused by a proton transfer from pinene to water clusters.

3.2 Formation of protonated water clusters

The distribution of protonated water clusters $(H_2O)_nH^+$ in the mixed pinene–water expansions has a maximum of n shifted toward higher values than expected for small clusters studied in this work. It was shown previously that electron ionization results in an extensive water cluster fragmentation,[20] which leads to a fast exponential decrease of the $(H_2O)_nH^+$ signal. However, this is not the case of the observed cluster distribution in the present experiment. To probe the neutral cluster size distribution, we employed the NaPI technique. The upper graphs of Fig. 3 show mass spectra after the EI and after NaPI for the conditions III. These conditions result in larger mixed clusters sizes, which could be measured by NaPI.

After EI, we observe a strong signal of pinene clusters, followed by the signal of mixed cluster cations. After NaPI with 315 nm photons, the only observed cluster distribution is that of water $(H_2O)_nNa^+$ clusters. NaPI is, therefore, selective for pure water clusters. This may have two reasons. The first is the reactivity of the solvated electron within the cluster as it has been already shown for several other systems.[32–34] The second reason may be evaporation of pinene after the Na doping or ionization. The energetics of the NaPI process enables evaporation of several molecules from the cluster (see *e.g.* ref. 35), which is negligible in large water clusters.[48] However, in a small system with weakly bound pinene this may result in preferential evaporation of pinene making our detection method blind for the mixed clusters.

The bottom part of Fig. 3 shows integrated peak intensities for $(H_2O)_nH^+$ and $(H_2O)_nNa^+$ ions after EI and NaPI, respectively. One can see that the distributions differ; the intensities of the cluster ions observed after NaPI significantly drop for $n > 7$ while the intensities of the cluster ions observed after EI continue to increase up to n = 9 and then only slowly decrease. As a result, also the mean cluster size is higher in the case of EI in comparison to NaPI, $\langle n \rangle \sim 11$ *vs.* $\langle n \rangle \sim 9$, respectively. For the water clusters, NaPI is ''fragmentation free''. Therefore, the cluster ions observed after EI can not originate purely from the ionization of neutral water clusters in the expansions. Rather, EI of mixed pinene–water clusters contributes to the observed signal of the pure protonated water cluster ions.

Our previous discussion about weak bonding between water and pinene suggests the explanation that these additional $(H_2O)_nH^+$ ions are formed by evaporation of pinene after ionization of water within the mixed cluster. According to our results presented in Fig. 5, the reorganization energy, which can

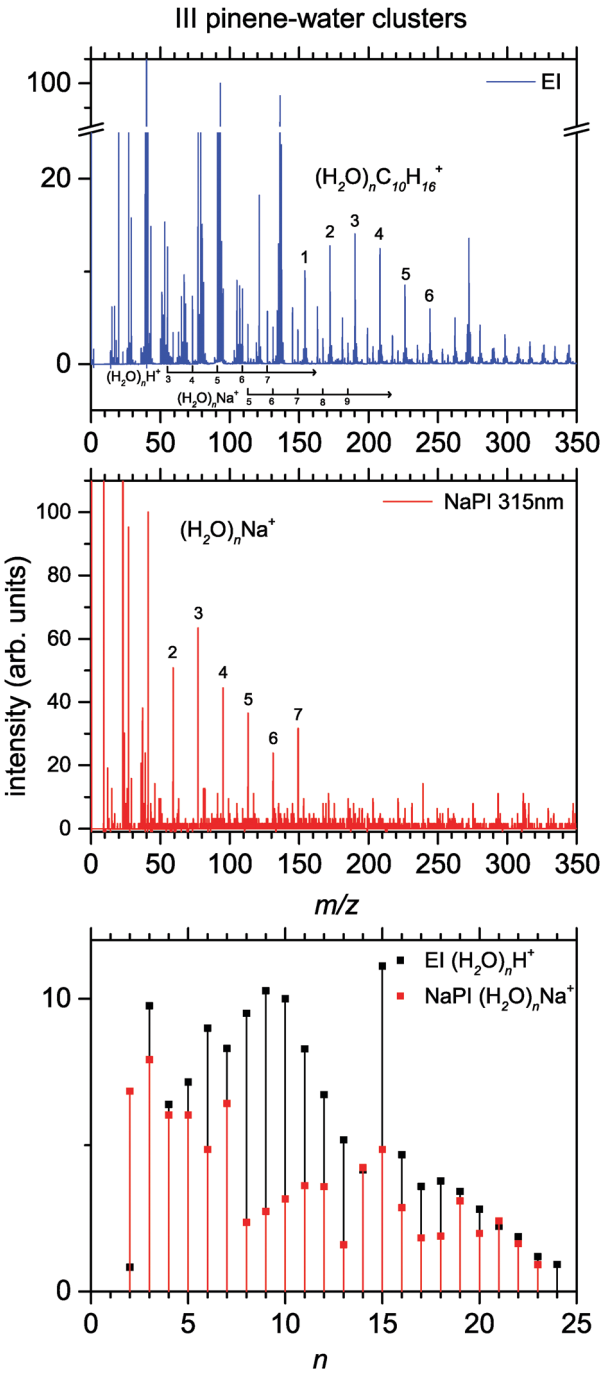

Fig. 3 Mass spectrum of cations formed after EI (top panel) or NaPI (middle panel) of mixed pinene–water clusters formed under expansion conditions III. Bottom panel shows dependence of the integrated ion signal for $(H_2O)_nH^+$ ions on cluster size n in comparison to the $(H_2O)_nNa^+$ signal after NaPI that resembles the distribution of neutral water clusters on expansion. The $(H_2O)_nNa^+$ signal was multiplied by 30 to compare the size distributions.

be released after ionization of pinene, is only 0.3 eV and slowly increases to ~1.1 eV for pinene with 8 water molecules attached. This increase is mainly due to the rearrangement of the water dipoles towards the pinene cation. The reorganization energy is lower than the energy released after ionization of water, which is gained by the formation of H_3O^+ cations.[49] This energy

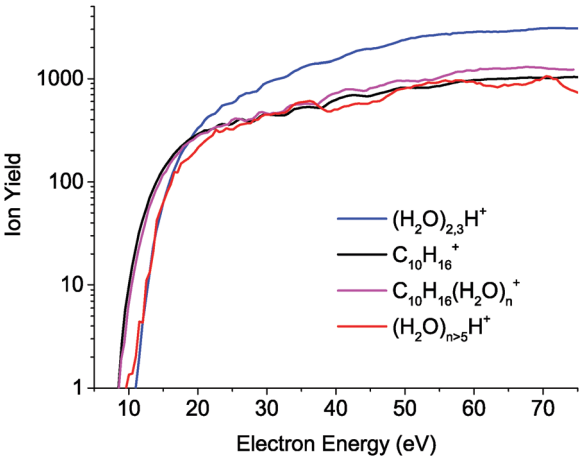

Fig. 4 Electron energy dependent ion yields for selected ions formed after EI to mixed pinene–water clusters at expansion conditions II.

release followed by orientation of water dipoles towards H_3O^+ may result in evaporation of pinene from the mixed clusters. Our calculated binding energy between the neutral pinene and neutral water amounts to about 0.2 eV, similar to the water–water binding energy in water dimers.[50] For larger clusters the value of binding energy oscillates around 0.3 eV (see ESI†), which is approximately half of the water–water binding energy (see Fig. 2). The energetics, therefore, supports the hypothesis that, after the ionization of pinene within the cluster, the pinene remains bound to the cluster, but it may easily evaporate after the ionization of water.

To test this hypothesis, we measured electron energy dependent ion yields for selected ionic species. The yields, measured at conditions II, are shown in Fig. 4. We can observe similar ionization yields for both the pinene $C_{10}H_{16}^+$ and mixed pinene–water $(H_2O)_nC_{10}H_{16}^+$ cluster cations. The ionization yield for small water clusters $(H_2O)_{2,3}H^+$ is shifted towards higher energies due to the higher ionization energy of water. Surprising is then the shape of the curve for larger water clusters $(H_2O)_{n>5}H^+$, in the region dominated by the ionization of mixed clusters identified by NaPI experiments. We can see that even though the threshold is shifted towards higher energies, the shape of the curve follows rather the pinene ionization yield than the water ionization yield. In the mixed clusters containing pinene and ~10 water molecules, the ionization of pinene is much more probable than the ionization of water. The observed increase in the protonated water cluster ion signal is therefore not caused by ionization of water in the mixed cluster and evaporation of pinene but occurs after primary ionization of pinene. The mechanism of the process is proposed on the basis of *ab initio* simulations in the next section.

3.3 Mechanism of charge transfer from pinene to the water cluster

There are two possible options of how the charge can be transferred from the pinene cation to the water cluster: electron transfer or proton transfer.

Electron transfer. While the energy of the ionized pinene is well below the energy of the ionized water clusters, thermal

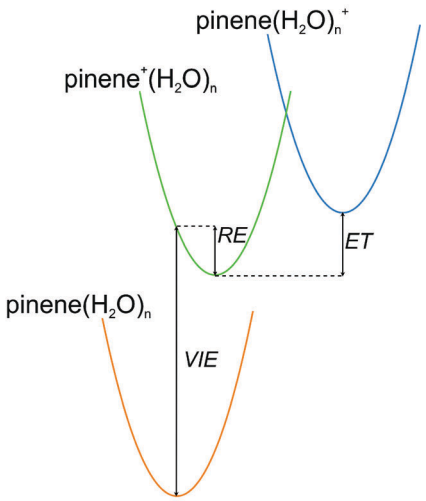

n	*VIE* [eV]	*RE* [eV]	*ET* [eV]
0	8.20	0.31	
1	8.45	0.80	
2	8.48	0.98	4.14
3	8.50	1.11	3.60
4	8.41	1.09	3.70
5	8.47	1.19	3.07
6	8.33	1.02	3.28
7	8.53	1.35	3.32
8	8.50	1.17	3.04

Fig. 5 Marcus-type diagram for the electron transfer process explaining the relationship between vertical ionization energy (VIE), reorganization energy (RE) and electron transfer energy (ET). The table lists the energies calculated at the BMK/6-31++g** level for different numbers of water molecules *n* in the mixed pinene–water cluster $C_{10}H_{16}(H_2O)_n^+$.

fluctuations might lead to geometries where this is no more true. When the systems appear in geometries where the two diabatic states (with charge on pinene and charge on water clusters) will cross each other, the electron transfer (ET) can take place. We can then estimate the energetics for the electron transfer process (see also Fig. 5 for a more detailed explanation of the ET process). The whole process can be expressed *via* the following scheme:

$$\begin{aligned} C_{10}H_{16}\cdot\cdot\cdot(H_2O)_n &\rightarrow C_{10}H_{16}^+\cdot\cdot\cdot(H_2O)_n \rightarrow C_{10}H_{16}\cdot\cdot\cdot(H_2O)_n^+ \\ &\rightarrow C_{10}H_{16}\cdot\cdot\cdot(H_2O)_{n-2}H_3O^+ + OH \end{aligned} \quad (1)$$

We have estimated the energy of the diabatic states with the help of the CDFT method. Upon the electron transfer, we always observe a proton transfer in the water moiety.[51] Once we optimized the structures of both diabatic states at the CDFT level, we re-optimized the structures with no charge constraint. The energies between the optimized initial structure and the structure upon ET are then compared in Fig. 5.

We observe that the ET process becomes energetically more feasible for larger clusters yet the reaction still requires more than 3 eV even for the largest molecular cluster (n = 8) considered. We can conclude that the electron transfer is not a viable route for the reaction.

Proton transfer. Alternatively, we may assume a process in which pinene deprotonates and the nascent hydrogen cation is

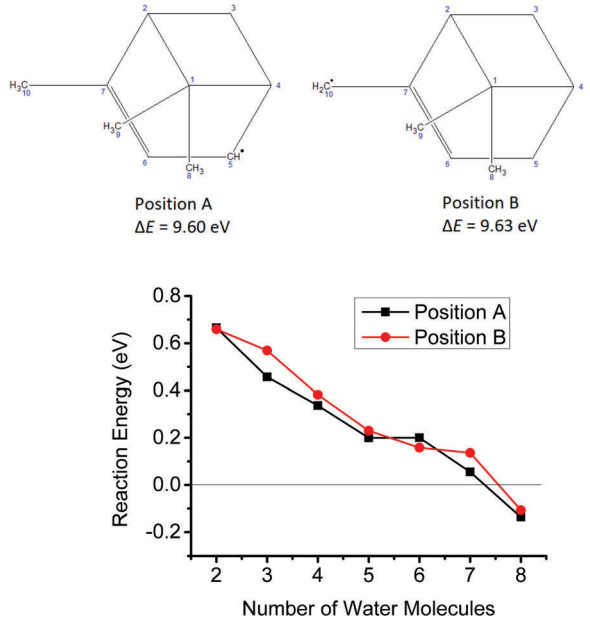

Fig. 6 Reaction energy for a proton transfer (PT) from pinene to water, showing exothermicity of the PT reaction for more than six water molecules. The calculations were performed for two deprotonation sites of pinene, marked in the structures in the upper right corner at the BMK/6-31++g** level.

then solvated by the water cluster. The process can be described as:

$$C_{10}H_{16}\cdots(H_2O)_n \rightarrow C_{10}H_{16}^{+}\cdots(H_2O)_n \rightarrow C_{10}H_{15}\cdots(H_2O)_{n-1}H_3O^{+} \quad (2)$$

We begin with identification of the weakest C–H bonds in the pinene, see Fig. 6. The proton will leave most likely from the 5th or 10th carbon on the pinene skeleton, leaving behind a structure with a stable allyl radical in both cases. The energy for the deprotonation amounts to about 9.6 eV. This large energy could be, however, easily compensated by the proton solvation energy in the liquid phase (amounting to about 11.5 eV).[52] The question immediately arises, what is the smallest size where we can observe this process in molecular clusters.

The size dependence of the reaction energy for the proton transfer is shown in Fig. 6. We observe a gradual decrease of the energy with increasing cluster size for both deprotonation sites considered. Importantly, the energies are much lower than those observed for the ET process and the reaction becomes exothermic for $n = 8$. This number seems to be in a nice agreement with the experimentally observed result.

At this moment, we cannot comment on the rate of such a process. However, there is enough time in the cluster beam for crossing the energy barrier for the proton transfer, especially considering the elevated ''temperatures'' in the cluster system upon the ionization.

3.4 Proton transfer *vs.* direct ionization of water

The proton transfer reaction is of particular importance for the stabilization of ionized water clusters.

Direct ionization of water clusters always results in the formation of protonated water cluster cations, independent of the ionization approach.[26,53,54] The reason is a fast proton transfer between the initially ionized H_2O^+ and neighboring water molecule occurring within less than 100 fs[51,55,56] and forming very stable H_3O^+. This process is purely exothermic,[51] and results in OH release and extensive fragmentation of the formed cluster cation.[20] The fragmentation of water clusters can be quenched in rare gas matrices,[26,57–59] however, not affecting the initial proton transfer reaction.[60,61]

Formation of ionized water clusters *via* ionization of pinene in the present case of heterogeneous pinene–water clusters is completely different. First, our calculations for the electron transfer process demonstrate that the ionization of pinene cannot result in the formation of a H_2O^+ cation. This is important, because the formation of H_2O^+ would enable the same fast and highly exothermic proton transfer as in the described case of direct ionization of water. Second, the release of the proton from pinene requires more energy than is gained by the formation of an H_3O^+ cation in the gas phase. For small clusters, the proton transfer will, therefore, not occur. The energy gained by ionization will be primarily used in the relatively slow process of water reorientation around the pinene cation and we will observe mainly pinene or mixed pinene–water cluster cations. Fig. 6 indicates that for the clusters with more than 7 molecules the proton transfer can proceed yet the process is not accompanied by evaporation of water. The binding energy of water in larger protonated clusters is about 0.4 eV.[62] The trend of the reaction energy curve depicted in Fig. 6 indicates that the first molecules may start to evaporate from clusters with more than 13 molecules. Besides, part of the energy released from the proton transfer process is removed by the pinene fragment leaving the cluster after the proton transfer and in such large water clusters the evaporation will be in strong competition with the internal energy redistribution. Proton transfer from pinene therefore represents a gentle pathway to ionized water clusters in contrast to proton transfer from water. Such stable protonated water clusters may then initiate further nucleation in a water rich atmosphere.[63,64]

4 Conclusions

We explored small mixed pinene–water clusters by EI and NaPI mass spectrometry. We show a protective effect of an environment on the pinene fragmentation after EI, which is more pronounced for homogeneous clusters. In mixed clusters, pinene is rather weakly bound to the water cluster.

The most important observation is that some of the protonated water cluster cations $(H_2O)_nH^+$ are formed by pinene ionization within the mixed clusters. *Ab initio* modelling illuminates the mechanism as proton transfer from pinene to water. The energy required for charge transfer from the pinene moiety with low ionization potential ($\sim$8.5 eV) to the water moiety with high ionization potential ($\sim$12 eV) is then supplied by proton solvation in water. Consequently, proton transfer is an endo- to

slightly exo-thermic process, depending on the number of water molecules in the mixed cluster. Ionization with pinene represents a route for a gentle protonation of water clusters. This pathway contrasts with the direct ionziation of pure water clusters characterized by a large excess energy and massive fragmentation.[20]

The threshold character of the proton transfer reaction with respect to the number of water molecules in the cluster enables experimental studies of the proton solvation at the nanoscale. Previously, cluster mass spectrometry has been successively used to probe phase transitions,[65,66] energy transfer to the solvent[67] or ion–solvent interaction at the nanoscale.[68] Combination of NaPI and EI methods in the present study allows us to directly experimentally determine the proton transfer contribution, as well as to demonstrate its dependence on the cluster size. Based on this approach, further experiments may be designed to provide a more complex picture of the proton transfer process.

Stable water cluster ions play an important role in atmospheric chemistry[69,70] and the proton transfer from pinene may be particularly relevant for the cloud nucleation induced by biogenic emissions.

Conflicts of interest

There are no conflicts to declare.

Acknowledgements

We would like to dedicate this article to Professor Mike Ashfold. This work has been supported by the Czech Science Foundation grant number 16-10995Y and Czech–French cooperation programme PHC Barrande, project 7AMB17FR047, (Fr) 38079PL. MF, PS and JP thank the Czech Science Foundation, grant number 17-04068S.

References

1 C. Geron, R. Rasmussen, R. R. Arnts and A. Guenther, *Atmos. Environ.*, 2000, **34**, 1761–1781.

2 B. Yuan, Z. Wang, X. Yue, F. Yu, C. Xie and S. Yu, *Renewable Energy*, 2018, **123**, 218–226.

3 M. G. Sobacchi, A. V. Saveliev, A. A. Fridman, A. F. Gutsol and L. A. Kennedy, *Plasma Chem. Plasma Process.*, 2003, **23**, 347–370.

4 S. Mellouli, L. Bousekkine, A. B. Theberge and W. T. S. Huck, *Angew. Chem., Int. Ed.*, 2012, **51**, 7981–7984.

5 J. Tröstl, W. K. Chuang, H. Gordon, M. Heinritzi, C. Yan, U. Molteni, L. Ahlm, C. Frege, F. Bianchi, R. Wagner, M. Simon, K. Lehtipalo, C. Williamson, J. S. Craven, J. Duplissy, A. Adamov, J. Almeida, A.-K. Bernhammer, M. Breitenlechner, S. Brilke, A. Dias, S. Ehrhart, R. C. Flagan, A. Franchin, C. Fuchs, R. Guida, M. Gysel, A. Hansel, C. R. Hoyle, T. Jokinen, H. Junninen, J. Kangasluoma, H. Keskinen, J. Kim, M. Krapf, A. Kürten, A. Laaksonen, M. Lawler, M. Leiminger, S. Mathot, O. Mähler, T. Nieminen, A. Onnela, T. Petäjä, F. M. Piel, P. Miettinen, M. P. Rissanen, L. Rondo, N. Sarnela, S. Schobesberger, K. Sengupta, M. Sipilä, J. N. Smith, G. Steiner, A. Tomé, A. Virtanen, A. C. Wagner, E. Weingartner, D. Wimmer, P. M. Winkler, P. Ye, K. S. Carslaw, J. Curtius, J. Dommen, J. Kirkby, M. Kulmala, I. Riipinen, D. R. Worsnop, N. M. Donahue and U. Baltensperger, *Nature*, 2016, **533**, 527–531.

6 F. Riccobono, S. Schobesberger, C. E. Scott, J. Dommen, I. K. Ortega, L. Rondo, J. Almeida, A. Amorim, F. Bianchi, M. Breitenlechner, A. David, A. Downard, E. M. Dunne, J. Duplissy, S. Ehrhart, R. C. Flagan, A. Franchin, A. Hansel, H. Junninen, M. Kajos, H. Keskinen, A. Kupc, A. Kürten, A. N. Kvashin, A. Laaksonen, K. Lehtipalo, V. Makhmutov, S. Mathot, T. Nieminen, A. Onnela, T. Petäjä, A. P. Praplan, F. D. Santos, S. Schallhart, J. H. Seinfeld, M. Sipilä, D. V. Spracklen, Y. Stozhkov, F. Stratmann, A. Tomé, G. Tsagkogeorgas, P. Vaattovaara, Y. Viisanen, A. Vrtala, P. E. Wagner, E. Weingartner, H. Wex, D. Wimmer, K. S. Carslaw, J. Curtius, N. M. Donahue, J. Kirkby, M. Kulmala, D. R. Worsnop and U. Baltensperger, *Science*, 2014, **344**, 717–721.

7 F. Bianchi, J. Tröstl, H. Junninen, C. Frege, S. Henne, C. R. Hoyle, U. Molteni, E. Herrmann, A. Adamov, N. Bukowiecki, X. Chen, J. Duplissy, M. Gysel, M. Hutterli, J. Kangasluoma, J. Kontkanen, A. Kürten, H. E. Manninen, S. Münch, O. Peräkylä, T. Petäjä, L. Rondo, C. Williamson, E. Weingartner, J. Curtius, D. R. Worsnop, M. Kulmala, J. Dommen and U. Baltensperger, *Science*, 2016, **352**, 1109–1112.

8 J. Kirkby, J. Duplissy, K. Sengupta, C. Frege, H. Gordon, C. Williamson, M. Heinritzi, M. Simon, C. Yan, J. Almeida, J. Tröstl, T. Nieminen, I. K. Ortega, R. Wagner, A. Adamov, A. Amorim, A.-K. Bernhammer, F. Bianchi, M. Breitenlechner, S. Brilke, X. Chen, J. Craven, A. Dias, S. Ehrhart, R. C. Flagan, A. Franchin, C. Fuchs, R. Guida, J. Hakala, C. R. Hoyle, T. Jokinen, H. Junninen, J. Kangasluoma, J. Kim, M. Krapf, A. Kürten, A. Laaksonen, K. Lehtipalo, V. Makhmutov, S. Mathot, U. Molteni, A. Onnela, O. Peräkylä, F. Piel, T. Petäjä, A. P. Praplan, K. Pringle, A. Rap, N. A. D. Richards, I. Riipinen, M. P. Rissanen, L. Rondo, N. Sarnela, S. Schobesberger, C. E. Scott, J. H. Seinfeld, M. Sipilä, G. Steiner, Y. Stozhkov, F. Stratmann, A. Tomé, A. Virtanen, A. L. Vogel, A. C. Wagner, P. E. Wagner, E. Weingartner, D. Wimmer, P. M. Winkler, P. Ye, X. Zhang, A. Hansel, J. Dommen, N. M. Donahue, D. R. Worsnop, U. Baltensperger, M. Kulmala, K. S. Carslaw and J. Curtius, *Nature*, 2016, **533**, 521–526.

9 R. Wagner, C. Yan, K. Lehtipalo, J. Duplissy, T. Nieminen, J. Kangasluoma, L. R. Ahonen, L. Dada, J. Kontkanen, H. E. Manninen, A. Dias, A. Amorim, P. S. Bauer, A. Bergen, A.-K. Bernhammer, F. Bianchi, S. Brilke, S. B. Mazon, X. Chen, D. C. Draper, L. Fischer, C. Frege, C. Fuchs, O. Garmash, H. Gordon, J. Hakala, L. Heikkinen, M. Heinritzi, V. Hofbauer, C. R. Hoyle, J. Kirkby, A. Kürten, A. N. Kvashnin, T. Laurila, M. J. Lawler, H. Mai, V. Makhmutov, R. L. Mauldin III,

U. Molteni, L. Nichman, W. Nie, A. Ojdanic, A. Onnela, F. Piel, L. L. J. Quéléver, M. P. Rissanen, N. Sarnela, S. Schallhart, K. Sengupta, M. Simon, D. Stolzenburg, Y. Stozhkov, J. Tröstl, Y. Viisanen, A. L. Vogel, A. C. Wagner, M. Xiao, P. Ye, U. Baltensperger, J. Curtius, N. M. Donahue, R. C. Flagan, M. Gallagher, A. Hansel, J. N. Smith, A. Tomé, P. M. Winkler, D. Worsnop, M. Ehn, M. Sipilä, V.-M. Kerminen, T. Petäjä and M. Kulmala, *Atmos. Chem. Phys.*, 2017, **17**, 15181–15197.

10 L. Stirnweis, C. Marcolli, J. Dommen, P. Barmet, C. Frege, S. M. Platt, E. A. Bruns, M. Krapf, J. G. Slowik, R. Wolf, A. S. H. Prévôt, U. Baltensperger and I. El-Haddad, *Atmos. Chem. Phys.*, 2017, **17**, 5035–5061.

11 J. A. Faust, J. P. S. Wong, A. K. Y. Lee and J. P. D. Abbatt, *Environ. Sci. Technol.*, 2017, **51**, 1405–1413.

12 O. Kostko, L. Belau, K. R. Wilson and M. Ahmed, *J. Phys. Chem. A*, 2008, **112**, 9555–9562.

13 Y. Li, X. Liu, X. Wang and N. Lou, *Chem. Phys. Lett.*, 1997, **276**, 339–345.

14 R. Pandey, M. Lalande, M. Ryszka, P. Limão-Vieira, N. J. Mason, J.-C. Poully and S. Eden, *Eur. Phys. J. D*, 2017, **71**, 190.

15 K. Khistyaev, A. Golan, K. B. Bravaya, N. Orms, A. I. Krylov and M. Ahmed, *J. Phys. Chem. A*, 2013, **117**, 6789–6797.

16 F. Berthias, L. Feketeová, H. Chermette, V. Forquet, C. Morell, H. Abdoul-Carime, B. Farizon, M. Farizon and T. D. Märk, *ChemPhysChem*, 2015, **16**, 3151–3155.

17 S. M. Craig, F. S. Menges, C. H. Duong, J. K. Denton, L. R. Madison, A. B. McCoy and M. A. Johnson, *Proc. Natl. Acad. Sci. U. S. A.*, 2017, **114**, E4706–E4713.

18 B. L. Yoder, K. B. Bravaya, A. Bodi, A. H. C. West, B. Sztáray and R. Signorell, *J. Chem. Phys.*, 2015, **142**, 114303.

19 J. H. Litman, B. L. Yoder, B. Schläppi and R. Signorell, *Phys. Chem. Chem. Phys.*, 2013, **15**, 940–949.

20 J. Lengyel, A. Pysanenko, V. Poterya, J. Kočišek and M. Fárník, *Chem. Phys. Lett.*, 2014, **612**, 256–261.

21 D. E. Folmer, E. S. Wisniewski, J. R. Stairs and A. W. Castleman, *J. Phys. Chem. A*, 2000, **104**, 10545–10549.

22 O. Kostko, T. P. Troy, B. Bandyopadhyay and M. Ahmed, *Phys. Chem. Chem. Phys.*, 2016, **18**, 25569–25573.

23 M. S. El-Shall, I. K. Attah and S. P. Platt, in *Noncovalent Interactions of Organic Ions with Polar Molecules in the Gas Phase*, ed. S. Scheiner, Springer International Publishing, Cham, 2015, pp. 443–469.

24 P. O. Momoh, A. M. Hamid, S. A. Abrash and M. Samy El-Shall, *J. Chem. Phys.*, 2011, **134**, 204315.

25 J. Kočišek, K. Grygoryeva, J. Lengyel, M. Fárník and J. Fedor, *Eur. Phys. J. D*, 2016, **70**, 98.

26 J. Kočišek, J. Lengyel, M. Fárník and P. Slavíček, *J. Chem. Phys.*, 2013, **139**, 214308.

27 C. Bobbert, S. Schütte, C. Steinbach and U. Buck, *Eur. Phys. J. D*, 2002, **19**, 183–192.

28 T. Zeuch and U. Buck, *Chem. Phys. Lett.*, 2013, **579**, 1–10.

29 A. H. C. West, B. L. Yoder, D. Luckhaus, C.-M. Saak, M. Doppelbauer and R. Signorell, *J. Phys. Lett.*, 2015, **6**, 1487–1492.

30 B. L. Yoder, J. H. Litman, P. W. Forysinski, J. L. Corbett and R. Signorell, *J. Phys. Lett.*, 2011, **2**, 2623–2628.

31 B. Schläppi, J. J. Ferreiro, J. H. Litman and R. Signorell, *Int. J. Mass Spectrom.*, 2014, **372**, 13–21.

32 J. Lengyel, A. Pysanenko, J. Kočišek, V. Poterya, C. C. Pradzynski, T. Zeuch, P. Slavíček and M. Fárník, *J. Phys. Lett.*, 2012, **3**, 3096–3101.

33 D. Šmídová, J. Lengyel, A. Pysanenko, J. Med, P. Slavíček and M. Fárník, *J. Phys. Lett.*, 2015, **6**, 2865–2869.

34 D. Šmídová, J. Lengyel, J. Kočišek, A. Pysanenko and M. Fárník, *Int. J. Mass Spectrom.*, 2017, **421**, 144–149.

35 J. Lengyel, A. Pysanenko, P. Rubovič and M. Fárník, *Eur. Phys. J. D*, 2015, **69**, 269.

36 A. D. Boese and J. M. L. Martin, *J. Chem. Phys.*, 2004, **121**, 3405.

37 M. Sodupe, J. Bertran, L. Rodríguez-Santiago and E. J. Baerends, *J. Phys. Chem. A*, 1999, **103**, 166–170.

38 B. Kaduk, T. Kowalczyk and T. Van Voorhis, *Chem. Rev.*, 2012, **112**, 321–370.

39 M. J. Frisch, G. W. Trucks, H. B. Schlegel, G. E. Scuseria, M. A. Robb, J. R. Cheeseman, G. Scalmani, V. Barone, B. Mennucci, G. A. Petersson, H. Nakatsuji, M. Caricato, X. Li, H. P. Hratchian, A. F. Izmaylov, J. Bloino, G. Zheng, J. L. Sonnenberg, M. Hada, M. Ehara, K. Toyota, R. Fukuda, J. Hasegawa, M. Ishida, T. Nakajima, Y. Honda, O. Kitao, H. Nakai, T. Vreven, J. A. Montgomery, Jr., J. E. Peralta, F. Ogliaro, M. Bearpark, J. J. Heyd, E. Brothers, K. N. Kudin, V. N. Staroverov, R. Kobayashi, J. Normand, K. Raghavachari, A. Rendell, J. C. Burant, S. S. Iyengar, J. Tomasi, M. Cossi, N. Rega, J. M. Millam, M. Klene, J. E. Knox, J. B. Cross, V. Bakken, C. Adamo, J. Jaramillo, R. Gomperts, R. E. Stratmann, O. Yazyev, A. J. Austin, R. Cammi, C. Pomelli, J. W. Ochterski, R. L. Martin, K. Morokuma, V. G. Zakrzewski, G. A. Voth, P. Salvador, J. J. Dannenberg, S. Dapprich, A. D. Daniels, Ö. Farkas, J. B. Foresman, J. V. Ortiz, J. Cioslowski and D. J. Fox, *Gaussian 09 Revision E.01*, Gaussian Inc., Wallingford CT, 2009.

40 Y. Shao, Z. Gan, E. Epifanovsky, A. T. Gilbert, M. Wormit, J. Kussmann, A. W. Lange, A. Behn, J. Deng, X. Feng, D. Ghosh, M. Goldey, P. R. Horn, L. D. Jacobson, I. Kaliman, R. Z. Khaliullin, T. Kuś, A. Landau, J. Liu, E. I. Proynov, Y. M. Rhee, R. M. Richard, M. A. Rohrdanz, R. P. Steele, E. J. Sundstrom, H. L. Woodcock III, P. M. Zimmerman, D. Zuev, B. Albrecht, E. Alguire, B. Austin, G. J. O. Beran, Y. A. Bernard, E. Berquist, K. Brandhorst, K. B. Bravaya, S. T. Brown, D. Casanova, C.-M. Chang, Y. Chen, S. H. Chien, K. D. Closser, D. L. Crittenden, M. Diedenhofen, R. A. DiStasio Jr., H. Do, A. D. Dutoi, R. G. Edgar, S. Fatehi, L. Fusti-Molnar, A. Ghysels, A. Golubeva-Zadorozhnaya, J. Gomes, M. W. Hanson-Heine, P. H. Harbach, A. W. Hauser, E. G. Hohenstein, Z. C. Holden, T.-C. Jagau, H. Ji, B. Kaduk, K. Khistyaev, J. Kim, J. Kim, R. A. King, P. Klunzinger, D. Kosenkov, T. Kowalczyk, C. M. Krauter, K. U. Lao, A. D. Laurent, K. V. Lawler, S. V. Levchenko, C. Y. Lin, F. Liu, E. Livshits, R. C. Lochan, A. Luenser, P. Manohar, S. F. Manzer, S.-P. Mao, N. Mardirossian, A. V. Marenich, S. A. Maurer, N. J. Mayhall, E. Neuscamman, C. M. Oana, R. Olivares-Amaya, D. P. O'Neill, J. A. Parkhill, T. M. Perrine, R. Peverati, A. Prociuk, D. R. Rehn,

E. Rosta, N. J. Russ, S. M. Sharada, S. Sharma, D. W. Small, A. Sodt, T. Stein, D. Stück, Y.-C. Su, A. J. Thom, T. Tsuchimochi, V. Vanovschi, L. Vogt, O. Vydrov, T. Wang, M. A. Watson, J. Wenzel, A. White, C. F. Williams, J. Yang, S. Yeganeh, S. R. Yost, Z.-Q. You, I. Y. Zhang, X. Zhang, Y. Zhao, B. R. Brooks, G. K. Chan, D. M. Chipman, C. J. Cramer, W. A. Goddard III, M. S. Gordon, W. J. Hehre, A. Klamt, H. F. Schaefer III, M. W. Schmidt, C. D. Sherrill, D. G. Truhlar, A. Warshel, X. Xu, A. Aspuru-Guzik, R. Baer, A. T. Bell, N. A. Besley, J.-D. Chai, A. Dreuw, B. D. Dunietz, T. R. Furlani, S. R. Gwaltney, C.-P. Hsu, Y. Jung, J. Kong, D. S. Lambrecht, W. Liang, C. Ochsenfeld, V. A. Rassolov, L. V. Slipchenko, J. E. Subotnik, T. V. Voorhis, J. M. Herbert, A. I. Krylov, P. M. Gill and M. Head-Gordon, *Mol. Phys.*, 2015, **113**, 184–215.

41 S. Stein, in *NIST Chemistry WebBook, NIST Standard Reference Database Number 69*, ed. P. Linstrom and W. Mallard, National Institute of Standards and Technology, Gaithersburg MD, 2017, p. 20899.

42 D. Kubala, E. Drage, A. Al-Faydhi, J. Kočišek, P. Papp, V. Matejčík, P. Mach, J. Urban, P. Limäo-Vieira, S. Hoffmann, Š. Matejčík and N. Mason, *Int. J. Mass Spectrom.*, 2009, **280**, 169–173.

43 S. Maclot, M. Capron, R. Maisonny, A. Ławicki, A. Méry, J. Rangama, J.-Y. Chesnel, S. Bari, R. Hoekstra, T. Schlathölter, B. Manil, L. Adoui, P. Rousseau and B. A. Huber, *ChemPhysChem*, 2011, **12**, 930–936.

44 P. Markush, P. Bolognesi, A. Cartoni, P. Rousseau, S. Maclot, R. Delaunay, A. Domaracka, J. Kocisek, M. C. Castrovilli, B. A. Huber and L. Avaldi, *Phys. Chem. Chem. Phys.*, 2016, **18**, 16721–16729.

45 M. Neustetter, M. Mahmoodi-Darian and S. Denifl, *J. Am. Soc. Mass Spectrom*, 2017, **28**, 866–872.

46 I. Fichan, C. Larroche and J. B. Gros, *J. Chem. Eng. Data*, 1999, **44**, 56–62.

47 S. Maheshwary, N. Patel, N. Sathyamurthy, A. D. Kulkarni and S. R. Gadre, *J. Phys. Chem. A*, 2001, **105**, 10525–10537.

48 P. W. Forysinski, P. Zielke, D. Luckhaus, J. Corbett and R. Signorell, *J. Chem. Phys.*, 2011, **134**, 094314.

49 B. C. Garrett, D. A. Dixon, D. M. Camaioni, D. M. Chipman, M. A. Johnson, C. D. Jonah, G. A. Kimmel, J. H. Miller, T. N. Rescigno, P. J. Rossky, S. S. Xantheas, S. D. Colson, A. H. Laufer, D. Ray, P. F. Barbara, D. M. Bartels, K. H. Becker, K. H. Bowen, S. E. Bradforth, I. Carmichael, J. V. Coe, L. R. Corrales, J. P. Cowin, M. Dupuis, K. B. Eisenthal, J. A. Franz, M. S. Gutowski, K. D. Jordan, B. D. Kay, J. A. LaVerne, S. V. Lymar, T. E. Madey, C. W. McCurdy, D. Meisel, S. Mukamel, A. R. Nilsson, T. M. Orlando, N. G. Petrik, S. M. Pimblott, J. R. Rustad, G. K. Schenter, S. J. Singer, A. Tokmakoff, L.-S. Wang and T. S. Zwier, *Chem. Rev.*, 2005, **105**, 355–390.

50 F. N. Keutsch and R. J. Saykally, *Proc. Natl. Acad. Sci. U. S. A.*, 2001, **98**, 10533–10540.

51 O. Svoboda, D. Hollas, M. Ončák and P. Slavíček, *Phys. Chem. Chem. Phys.*, 2013, **15**, 11531–11542.

52 C. P. Kelly, C. J. Cramer and D. G. Truhlar, *J. Phys. Chem. B*, 2006, **110**, 16066–16081.

53 F. Dong, S. Heinbuch, J. J. Rocca and E. R. Bernstein, *J. Chem. Phys.*, 2006, **124**, 224319.

54 L. Belau, K. R. Wilson, S. R. Leone and M. Ahmed, *J. Phys. Chem. A*, 2007, **111**, 10075–10083.

55 O. Marsalek, C. G. Elles, P. A. Pieniazek, E. Pluhařová, J. VandeVondele, S. E. Bradforth and P. Jungwirth, *J. Chem. Phys.*, 2011, **135**, 224510.

56 J. Chalabala, F. Uhlig and P. Slavíček, *J. Phys. Chem. A*, 2018, **122**, 3227–3237.

57 R. T. Jongma, Y. Huang, S. Shi and A. M. Wodtke, *J. Phys. Chem. A*, 1998, **102**, 8847–8854.

58 S. Denifl, F. Zappa, I. Mähr, F. Ferreira da Silva, A. Aleem, A. Mauracher, M. Probst, J. Urban, P. Mach, A. Bacher, O. Echt, T. Märk and P. Scheier, *Angew. Chem.*, 2009, **121**, 9102–9105.

59 A. Golan and M. Ahmed, *J. Phys. Lett.*, 2012, **3**, 458–462.

60 G. H. Gardenier, M. A. Johnson and A. B. McCoy, *J. Phys. Chem. A*, 2009, **113**, 4772–4779.

61 K. Mizuse and A. Fujii, *J. Phys. Chem. A*, 2013, **117**, 929–938.

62 K. Hansen, P. U. Andersson and E. Uggerud, *J. Chem. Phys.*, 2009, **131**, 124303.

63 S. Zamith, G. de Tournadre, P. Labastie and J.-M. L'Hermite, *J. Chem. Phys.*, 2013, **138**, 034301.

64 I. Braud, J. Boulon, S. Zamith and J.-M. L'Hermite, *J. Phys. Chem. A*, 2015, **119**, 6017–6023.

65 M. Schmidt and B. von Issendorff, *J. Chem. Phys.*, 2012, **136**, 164307.

66 J. Boulon, I. Braud, S. Zamith, P. Labastie and J.-M. L'Hermite, *J. Chem. Phys.*, 2014, **140**, 164305.

67 J. Poštulka, P. Slavíček, J. Fedor, M. Fárník and J. Kočišek, *J. Phys. Chem. B*, 2017, **121**, 8965–8974.

68 W. A. Donald, R. D. Leib, J. T. O'Brien, A. I. S. Holm and E. R. Williams, *Proc. Natl. Acad. Sci. U. S. A.*, 2008, **105**, 18102–18107.

69 S. Aloisio and J. S. Francisco, *Acc. Chem. Res.*, 2000, **33**, 825–830.

70 V. Vaida, *J. Chem. Phys.*, 2011, **135**, 020901.